EXPERIMENTAL STUDY ON FLUID MOTION OF WATER VORTEX FOLLOWING KEPLER'S LAWS

Wang Yi
vortexhuhu@gmail.com

June 29, 2025

ABSTRACT

This study aims to verify through physical experiments whether the fluid motion laws in a water vortex system conform to Kepler's laws of planetary motion. Specifically, by quantitatively analyzing the orbital parameters of rotating spheres in the vortex, it examines the applicability of Kepler's third law (the ratio of the cube of the semi-major axis of the orbit to the square of the period is a constant) in fluid mechanics scenarios. It also explores the potential of water vortices as a macroscopic physical model for simulating the laws of celestial body motion.

***K*eywords** Water Vortex; Kepler's Laws; Machine Vision; Fluid Motion

1 Introduction

Inspired by the universality of Kepler's laws in celestial systems, this study attempts to apply machine vision technology (industrial camera + VisionMaster software) to water vortex dynamics experiments, exploring the isomorphism between fluid motion and celestial motion through the following approaches:

- Quantitative Verification: Using a magnetic stirrer to generate stable axisymmetric water vortices, measuring orbital parameters of multiple sets of suspended balls, and analyzing the degree of coincidence between the R^3/T^2 ratio and Kepler's third law, so as to provide experimental evidence for whether there are orbital laws similar to celestial bodies in fluid systems.
- Method Optimization: Aiming at the problem of vortex stability in traditional research, a dual screening strategy of "trajectory repeatability constraint method" and "energy conservation verification method" is proposed, providing a new technical path for vortex energy monitoring in dynamic equilibrium.
- Model Expansion: If the experiment is verified, the water vortex system can be used as a macroscopic physical model with both cost-effectiveness and visualization advantages, providing a supplementary reference framework for the teaching demonstration and theoretical research of celestial motion laws.

2 Experimental Methods

2.1 Experimental Setup and Observation Methods

A magnetic stirrer was used to generate a stable axisymmetric water vortex. A yellow floating ball (Ball C) was placed at the center of the vortex as the central reference point, and red (Ball A) and blue (Ball B) floating balls were symmetrically arranged in the periphery as orbital observation objects. The motion trajectories of the balls were real-time captured by a machine vision system (equipped with an industrial camera, model: MV-CU120-10GC, with the lens vertically 50.0 cm away from the water surface). The distance data between the centers of the two balls and Ball C were recorded by VisionMaster software (Version: V5.3.1) at a frequency of 4.0±0.1 frames per second, so as to analyze the motion trajectories of Ball A (red) and Ball B (blue) in the vortex plane through pixel coordinates.

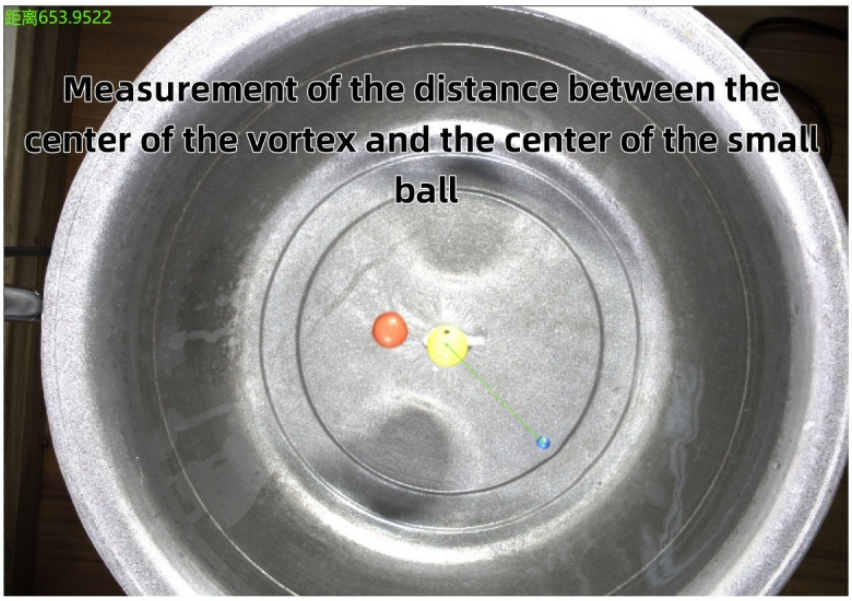
距离653.9522
Measurement of the distance between the center of the vortex and the center of the small ball


距离279.4191

2.2 Screening of Vortex Samples

The experiment requires a stable vortex with essentially constant energy. A stable vortex refers to one with minimal energy change per unit time, similar to a figure skater spinning on ice, which maintains short-term angular momentum conservation without extra assistance. However, for water vortices, due to the high viscosity of water, the energy dissipates extremely rapidly and the rotation speed drops sharply once the magnetic stirrer stops rotating.

To obtain a stable vortex or achieve a similar stable state, the magnetic stirrer was kept rotating at a constant speed to enable the vortex system to achieve a dynamic balance between energy input and viscous dissipation. Ideally, after the vortex stabilizes, the velocity and period of the balls in their respective orbits remain constant. In practice, energy fluctuations are inevitable during dynamic balance establishment, such as minor changes in surface tension affecting intermolecular forces and disturbing energy balance, or unstable energy transfer caused by flow pattern changes during the transition between laminar and turbulent flow. These fluctuations lead to continuous dynamic changes in the balls' orbital radii, increasing the difficulty of precise experimental data measurement.

To address this, two methods were proposed to obtain relatively stable water vortices:

Strategy 1: Trajectory Repeatability Constraint Method In the vortex experiment, the basic condition is set as follows: Balls A and B are started synchronously, and after each completing one circle of motion, both approximately return to their initial positions. Due to differences in motion radius and period, when Ball A finishes its first motion cycle, Ball B is still in the process of its first cycle of motion (with a time difference of about 2 - 10 seconds). In the experiment, the trajectory of Ball A is recorded by an industrial camera, and it is required that the trajectory of its second motion cycle basically coincides with that of the first cycle in space. According to the principles of fluid mechanics, when the energy of the vortex flow field is stable, the motion trajectories of the balls are similar in form; if the energy fluctuates, the trajectories will change. Subsequent comparison of trajectory forms helps screen out experimental samples with relatively stable vortex energy, thereby reducing measurement errors caused by energy fluctuations.

Strategy 2: Energy Conservation Verification Method Assuming that the period of Ball B is longer than that of Ball A, when Ball A shows an increase in orbital radius (R2) and an extension of the motion period (T2) in the second motion cycle, the ratio of R23/T22 to R13/T12 of the first cycle is calculated based on Kepler's third law. If the difference between the two ratios is within the allowable experimental error, it indicates that the total energy of the vortex system remains basically unchanged during this period, and this sample can be used as valid experimental data. This method provides a reliable basis for screening experimental data by establishing the correlation between ball motion parameters and vortex energy states.

3 Experimental Process

3.1 Precalibration

System Calibration

- Adjust the levelness of the experimental platform to ensure the camera's optical axis is vertically aligned with the vortex center, and complete the camera internal parameter calibration using a chessboard calibration plate. (as shown in the figure below)

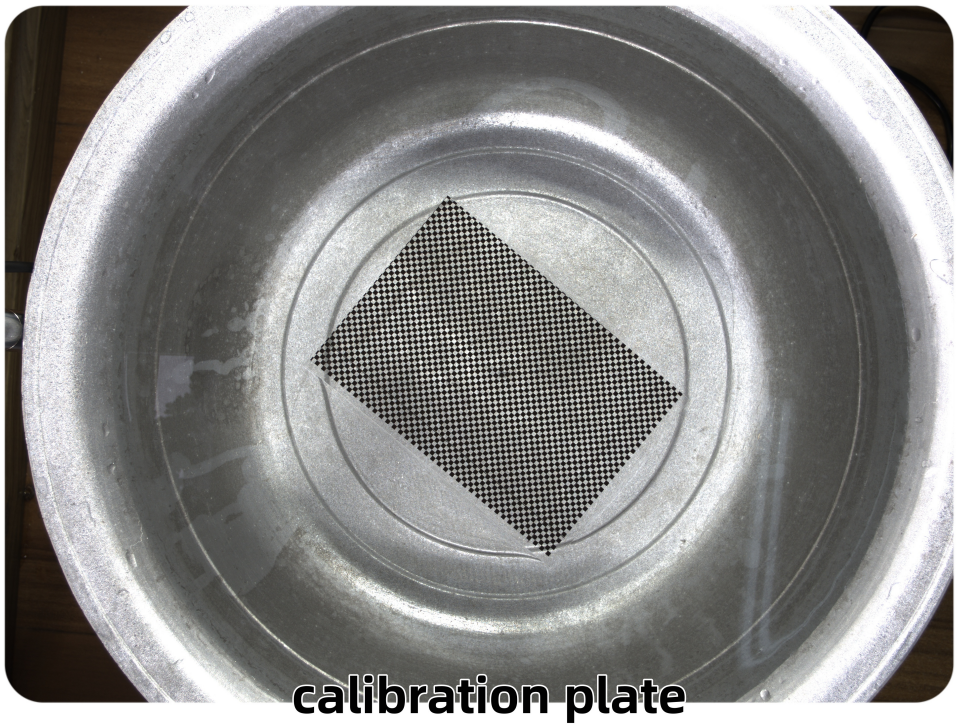

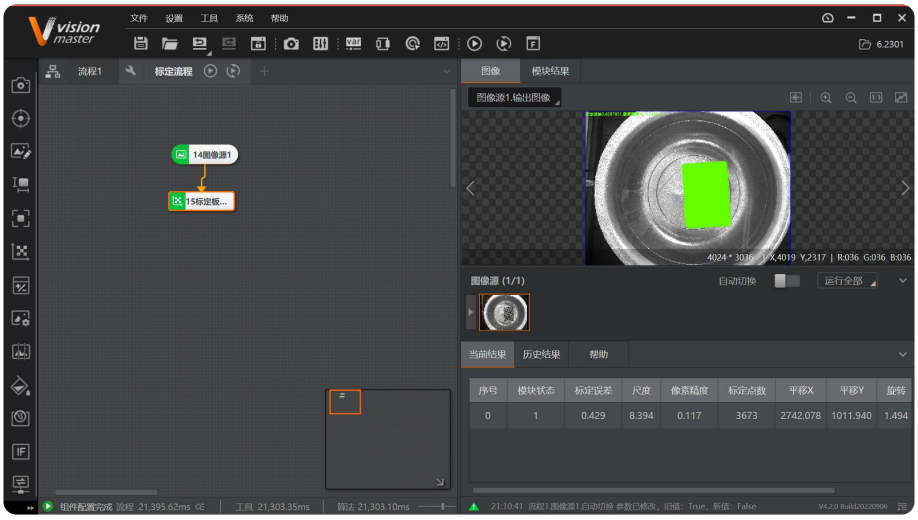

Calibration accuracy: 0.117mm

- After the calibration process was completed, a systematic measurement verification was carried out on the rectangular standard parts with known reference dimensions (length × width). Through multi-directional dynamic floating tests, a quantitative evaluation was conducted on the dimensional detection accuracy of the visual measurement system. The actual measurement data shows that for the length parameter of the rectangular standard object, the system's measured value is 100.247mm, while its actual reference dimension is 100.303mm. After calculation, the measurement error is controlled at the level of 0.056mm . (as shown in the figure below)

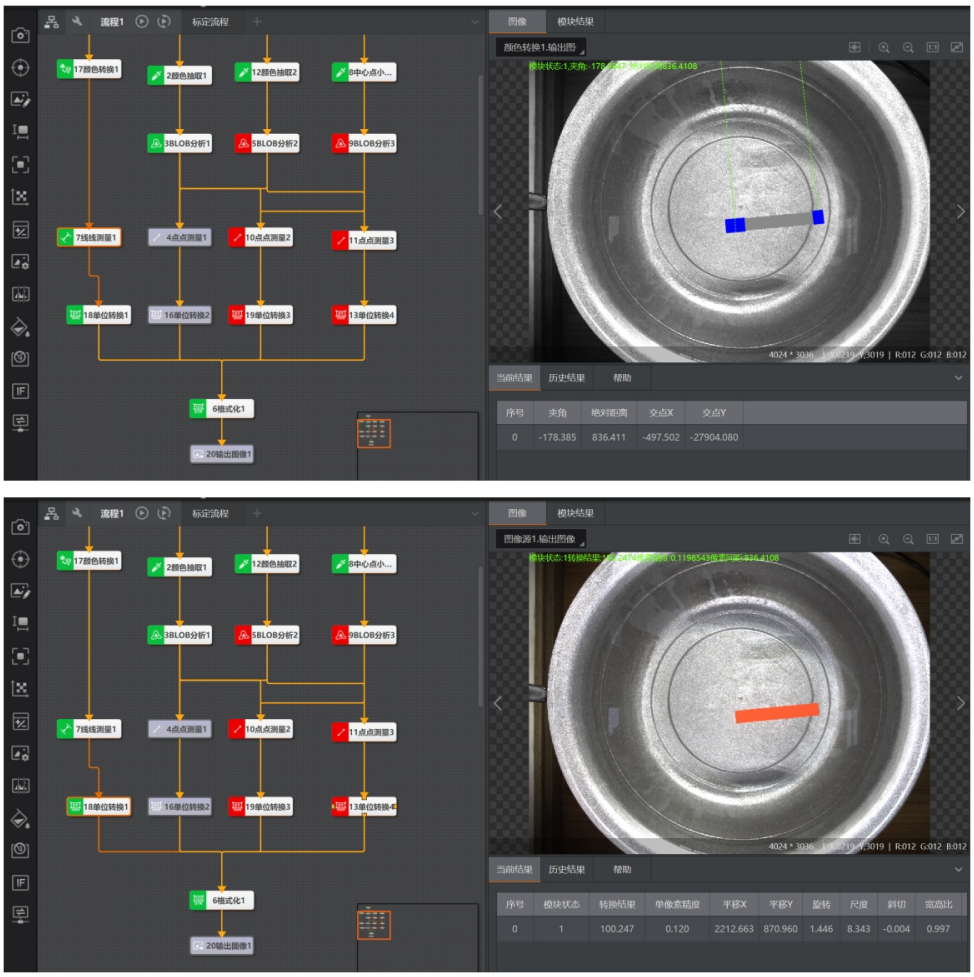

Environmental Control

- Configure a ring-shaped light supplement system to ensure the water surface imaging contrast ratio $\geq 60\%$ and reduce image noise.

- Maintain a constant stirrer rotation speed to keep the water level fluctuation amplitude <3 mm, ensuring the three balls are basically on the same horizontal plane.

3.2 Experimental Data Recording and Analysis

Through the video recording of VisionMaster, the central distance data of Ball A (red) and Ball B (blue) at different moments (based on 30 frames per second) were extracted. The typical sampling points are shown in the following table:

3.2.1 Data from the first group of experiments:

Ball A (Red)	Time in Video (30 Frames per Second)	Distance from Vortex Center (mm)	Ball B (Blue)	Time in Video (30 Frames per Second)	Distance from Vortex Center (mm)
Start	24s17f	50.843	Start	24s17f	86.205
	24s28f	50.959		24s28f	85.249
	25s14f	53.278		25s14f	84.192
	25s27f	65.052		25s27f	85.651
	26s07f	74.336		26s07f	86.429
	26s21f	74.568		26s21f	87.610
	27s05f	76.123		27s05f	88.758
	27s17f	76.610		27s17f	98.756
	28s15f	66.305		28s15f	95.175
	28s28f	63.382		28s28f	101.469
End of First Period	29s10f	52.84		29s10f	95.632
	29s25f	53.498		29s25f	86.45
	30s09f	48.576		30s09f	89.033
	30s21f	54.669		30s21f	84.164
	31s	54.175		31s	88.865
	31s22f	58.239		31s22f	89.654
	32s06f	49.964		32s06f	90.678
	32s19f	46.054	End of Period	32s13f	90.800

Parameter Calculation:

Period Determination

- Period of Ball A: 29s10f - 24s17f = 4.767s (1 second = 30 frames), so the calculated $T_A = 4.767s$.
- Period of Ball B: 32s13f - 24s17f = 7.867s, so the calculated $T_B = 7.867s$.

Calculation of R

- Method 1: The pixel coordinates of the small balls were recorded and their trajectories were exported. It can be observed that all trajectories are ellipses approximating circles. Origin software was used to perform circle fitting and ellipse fitting on the trajectories respectively. The former can obtain the radius of the circle, and the latter can obtain the semi - major axis of the ellipse. The radial parameter (R) values obtained by the two fitting methods are close. After comprehensive comparison, since the goodness of fit of circle fitting is higher and the deviation of the center is smaller, the circle fitting results are finally selected.The following are the trajectory fitting graphs of the red ball and blue ball, as well as R_A and R_B derived therefrom.

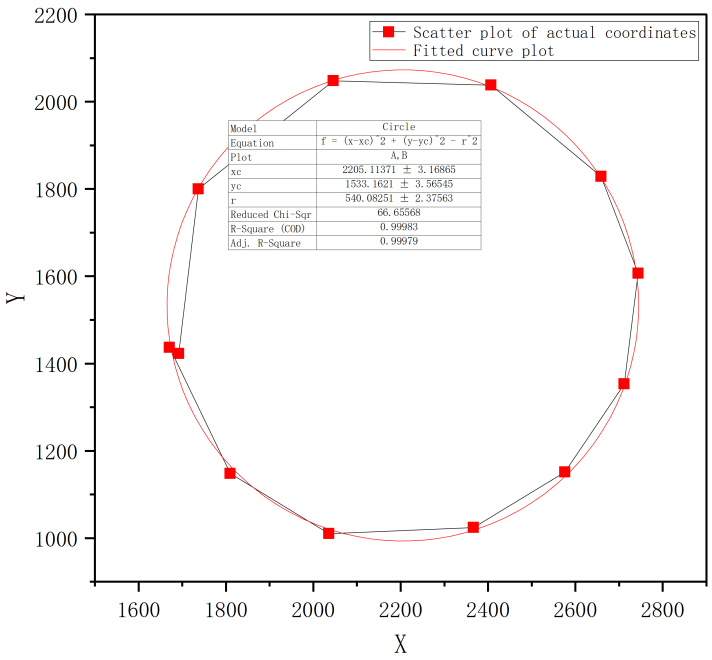

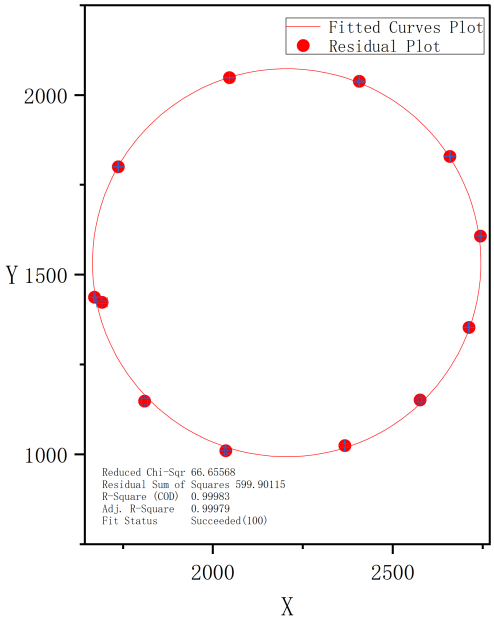

$R_A = 540.08251 \times 0.117 = 63.189$ mm (pixel distance × pixel accuracy)

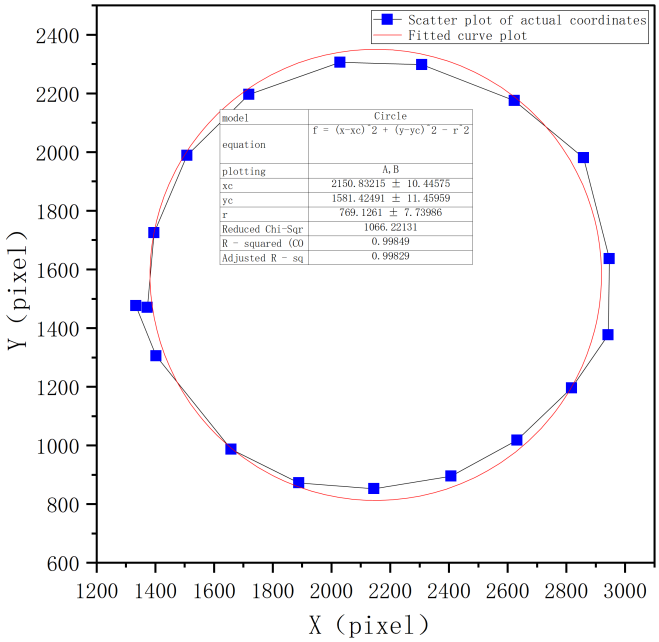

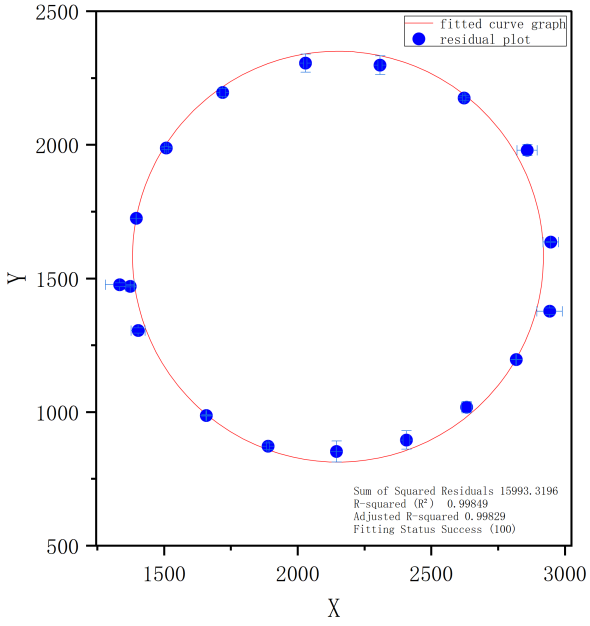

$R_B = 769.1261 \times 0.117 = 89.987$ mm (pixel distance × pixel accuracy)

- Method 2: Meanwhile, considering that the arithmetic mean method has good universality and operational convenience in processing irregular trajectory data, the arithmetic mean of multiple measurements was also adopted in the experiment as the characterization parameter of the radial distance (R). This method can accurately reflect the actual characteristics of the movement trajectory of the small balls and provide a supplementary quantitative basis for the experimental data.

  $R_A = 64.027$ mm

$R_B = 89.70977$ mm

Law Verification(fitting curve):

- Ball A: $R_A^3/T_A^2 = 63.189^3/4.767^2 = 11100\ (mm^3/s^2)$
- Ball B: $R_B^3/T_B^2 = 89.987^3/7.867^2 = 11770\ (mm^3/s^2)$

Law verification (arithmetic mean):

- Ball A: $R_A^3/T_A^2 = 11550.57\ (mm^3/s^2)$
- Ball B: $R_B^3/T_B^2 = 11665.03\ (mm^3/s^2)$

3.2.2 Data from the second group of experiments:

Ball A (Red)	Time in Video (30 Frames per Second)	Distance from Vortex Center (mm)	Ball B (Blue)	Time in Video (30 Frames per Second)	Distance from Vortex Center (mm)
Start	1min46s08f	76.088	Start	1min46s08f	58.994
	1min46s27f	71.545		1min46s27f	55.208
	1min47s06f	69.323		1min47s06f	55.549
	1min47s16f	70.695		1min47s16f	58.239
	1min47s28f	72.632		1min47s28f	60.901
	1min48s09f	77.492		1min48s09f	57.601
	1min48s22f	79.452		1min48s22f	56.231
	1min49s04f	79.106		1min49s04f	56.228
	1min49s14f	82.085		1min49s14f	54.498
	1min49s25f	82.021		1min49s25f	54.886
	1min50s08f	85.218	End of First Period	1min50s06f	55.338
	1min50s22f	86.052		1min50s22f	55.543
	1min51s05f	88.834		1min51s05f	58.210
	1min51s18f	92.347		1min51s18f	62.549
	1min52s05f	95.392		1min52s05f	66.214
	1min52s15f	95.053		1min52s15f	65.213
	1min53s01f	93.627		1min53s01f	63.882
	1min53s12f	91.809		1min53s12f	59.986
End of Period	1min53s25f	90.138		1min53s25f	57.761

Parameter Calculation:

Period Determination

- Period of Ball A: 1min53s25f - 1min46s08f = 7.57s (1 second = 30 frames), so $T_A = 7.57s$.
- Period of Ball B: 1min50s06f - 1min46s08f = 3.93s, so $T_B = 3.93s$.

Calculation of R (Arithmetic Mean)

- $$\begin{aligned} RA = &(76.088 + 71.545 + 69.323 + 70.695 + 72.632 + 77.492 + 79.452 \\ &+ 79.106 + 82.085 + 82.021 + 85.218 + 86.052 + 88.834 \\ &+ 92.347 + 95.392 + 95.053 + 93.627 + 91.809 + 90.138) \div 19 \\ = &83.1 \end{aligned}$$

- $$\begin{aligned} RB = &(58.994 + 55.208 + 55.549 + 58.239 + 60.901 + 57.601 + 56.231 \\ &+ 56.228 + 54.498 + 54.886 + 55.338) \div 11 \\ = &56.698 \end{aligned}$$

Law Verification

- For Ball A: $\frac{R_A^3}{T_A^2} = \frac{(83.1\text{ mm})^3}{(7.57\text{ s})^2} = \frac{573047.491\text{ mm}^3}{57.3049\text{ s}^2} = 10014.1\ (\text{mm}^3/\text{s}^2)$
- For Ball B: $\frac{R_B^3}{T_B^2} = \frac{56.698^3}{3.93^2} = 11800\ (\text{mm}^3/\text{s}^2)$

3.2.3 Data of the third group of experiments

Ball A (Red)	Time in Video (30 Frames per Second)	Distance from Vortex Center (mm)	Ball B (Blue)	Time in Video (30 Frames per Second)	Distance from Vortex Center (mm)
Start	23s29f	84.791	Start	23s29f	82.477
	24s14f	86.890		24s14f	82.616
	24s25f	86.304		24s25f	78.151
	25s07f	84.192		25s07f	77.147
	25s21f	82.876		25s21f	81.919
	26s03f	82.999		26s03f	88.119
	26s15f	81.977		26s15f	94.797
	27s	80.340		27s	98.517
	27s11f	79.251		27s11f	103.479
	27s23f	80.058		27s23f	103.631
	28s04f	76.158		28s04f	98.734
	28s18f	73.739		28s18f	91.840
	28s29f	71.207		28s29f	84.782
	29s11f	71.376		29s11f	87.245
	29s24f	71.458		29s24s	84.139
	30s06f	74.986		30s06f	81.251
End of Period	30s12f	80.000		30s19f	81.565
			End of Period	31s06f	83.084

Parameter Calculation:

Period Determination

- Period of Ball A: 30s12f - 23s29f = 6.43s, so $T_A = 6.43s$.
- Period of Ball B: 31s06f - 23s29f = 7.23s, so $T_B = 7.23s$.

Calculation of R (Arithmetic Mean) $R_A = 79.2$ mm, $R_B = 87.97$ mm.

Law Verification

- For Ball A: o For Ball A: $\frac{R_A^3}{T_A^2} = 12015.7\ (mm^3/s^2)$.
- For Ball B: $\frac{R_B^3}{T_B^2} = 13023.4\ (mm^3/s^2)$.

3.2.4 Data of the fourth group of experiments

Ball A (Red)	Time in Video (30 Frames per Second)	Distance from Vortex Center (mm)	Ball B(Blue)	Time in Video (30 Frames per Second)	Distance from Vortex Center (mm)
Start	23s12f	68.691	Start	23s12f	82.425
	24s	67.103		24s	81.668
	24s11f	63.076		24s11f	78.934
	24s24f	61.183		24s24f	77.432
	25s03f	62.350		25s03f	78.530
	25s15f	60.572		25s15f	87.516
	25s27f	58.790		25s27f	94.212
	26s11f	56.798		26s11f	99.325
	26s23f	60.699		26s23f	102.140
End of First Period	26s27f	70.12		26s27f	108.323
	27s01f	80.414		27s01f	115.865
	27s12f	70.250		27s12f	105.359
	27s24f	68.585		27s24f	111.313
	28s06f	64.555		28s06f	113.475
	28s16f	64.733		28s16f	111.342
	28s29f	70.759		28s29f	114.750
	29s08f	75.701		29s08f	109.739
	29s19f	82.647		29s19f	100.440
	29s28f	72.957		29s28f	97.710
	30s08f	75.733	End of Period	30s08f	83.479

r

Parameter Calculation:

Period Determination

- Period of Ball A: 26s27f - 23s12f = 3.5s, so $T_A = 3.5s$.
- Period of Ball B: 30s08f - 23s12f = 6.867s, so $T_B = 6.867s$.

Calculation of R (Arithmetic Mean) $R_A = 62.9382$ mm, $R_B = 97.7$ mm.

Law Verification

- For Ball A: $\frac{R_A^3}{T_A^2} = 20430\ (mm^3/s^2)$.
- For Ball B: $\frac{R_B^3}{T_B^2} = 19770\ (mm^3/s^2)$.

3.3 Experimental Errors

- The camera calibration error is 0.211 mm (the camera lens is approximately 50 cm away from the water surface, using a monocular camera).
- When the vortex rotates, there is a slight fluctuation in the water level. Therefore, it is necessary to keep the magnetic stirrer rotating at a constant and slow speed to minimize the water surface drop, and ensure that the centers of the three balls are basically on the same plane to reduce measurement errors.
- In the experiment, the vortex system achieves a short-term dynamic equilibrium between energy input and viscous dissipation. During the equilibrium process, there will be energy fluctuations, which lead to changes in the vortex energy. Consequently, the orbit or period of the small balls will change accordingly. This unstable state is the main cause of errors in the experimental results.

4 Experimental Summary

Through repeated experiments, an exploratory study was conducted on the potential correlation between the hydrodynamic behavior of the water vortex system and the laws of celestial motion. The experimental data show that the measured orbital parameters of the peripheral suspended spheres are consistent with the theoretical expectations of Kepler's third law — the calculated results of R^3/T^2 for each sphere all fall within the range of experimental errors. However, the universality of this model still needs to be verified under more working conditions (such as different vortex intensities and different fluid media).

Experimental observations indicate that there is a significant correlation between the rotational speed of the magnetic stirrer and the energy state of the vortex system: when the rotational speed of the stirrer increases, the angular velocity of the magnetic stir bar increases accordingly, which directly drives the overall rotational speed of the water vortex to increase, and the enhancement of the vortex rotational speed can be regarded as an intuitive characterization of the increase in the system's energy. Specific experimental data show that under the working condition of a rotational speed of 280 revolutions per minute (Experiment 1), the measured Kepler constant K_1 is 11000 mm^3/s^2; when the rotational speed is increased to 310 revolutions per minute (Experiment 4), the corresponding Kepler constant K_4 increases to 20000 mm^3/s^2. The above results reveal that the energy level of the water vortex system is positively correlated with the Kepler constant, that is, the higher the energy of the vortex, the larger the corresponding R^3/T^2 ratio (Kepler constant).

The Kepler constant of Experiment 2 shows a relatively larger deviation (compared with other groups). This is because there is a significant difference between the starting position (76.088) and the ending position of the first cycle (90.138) of the red ball. Its trajectory presents an open spiral shape accompanied by vortex energy fluctuations, which makes it difficult to accurately determine the cycle time. Therefore, when selecting experimental samples, priority should be given to those where the starting position is the same as or close to the ending position of the cycle.

In orbital observations, it was found that while the peripheral spheres perform revolution, they are accompanied by significant spin and precession phenomena. Particularly interestingly, an Earth-Moon system-like composite motion pattern was observed: Ball A orbits along the main track of the vortex center, and Ball B orbits around Ball A as a secondary center. This dynamic behavior exhibits isomorphism with the multi-level motion architecture of satellites-planets-stars in celestial systems.

Meanwhile, optimizing the stability of the flow field is the key to improving the accuracy of experimental verification. Using a low-viscosity liquid as the experimental medium can significantly slow down the energy dissipation rate of the vortex. Under this condition, even if the stirrer stops rotating, the vortex can maintain a stable rotation speed and continue to rotate. This low-energy-consumption motion state can more realistically simulate the motion environment of celestial bodies in space, thereby obtaining more accurate and reliable experimental data.

5 Attachment:

Experiment Video 1 (Recording of the first group's experiment process, corresponding to the data in Table 1):

`https://youtu.be/SwqySjDzqR0`

Experiment Video 2:

`https://youtu.be/LE-pxjYOjzA`

Experiment Video 3:

https://youtu.be/LE-pxjYOjzA

Experiment Video 4:

https://youtu.be/LWo3ST4B0k0